JETIR.ORG ISSN: 2349-5162 | ESTD Year : 2014 | Monthly Issue
JOURNAL OF EMERGING TECHNOLOGIES AND INNOVATIVE RESEARCH (JETIR)
An International Scholarly Open Access, Peer-reviewed, Refereed Journal

DFT study of four isolated compounds form leaves of *Coccinia grandis (L.)* which are explore to medicinal application

Sanjay V. Chavan*

Associate Professor

Department of Chemistry, Rani Laxmibai Mahavidyalaya, Parola, 425111, Jalgaon, MS. India

EmailAddress: sanjayvchavan48@gmail.com

Mob.:+919922085588

***ABSTRACT*:** Plant-source bioactive compounds are crucial potential drugs against therapeutic dieses. The present study investigated four bioactive compounds isolated from Wrightia tinctoria R.Br. leaves, named compound -1, compound -2, compound-3, and compound-4. These compounds are identified by TLC and separated by HPLC, while compounds are characterised by UV, FT-IR, 1HNMR, 13CNMR, and mass spectroscopy. All four compounds exhibit potent antibacterial and antioxidant activity. MEP, EHOMO, ELUMO, and global properties of all isolated compounds are computed by DFT methods. The molecular docking study showed that most of the isolated compounds, especially compounds 3 and 4, interact strongly with 4PYP, with the highest binding energies maintaining the high cytotoxic activity of these compounds against HepG-2 cells in the experimental part. Bioactivity Score, Drug-Likeness, and ADMET studies supported the potential biological activities of most isolated compounds, especially compounds 3 and 4, and also created attention for developing them to act as good candidates.

***Keywords*: Bioactive, DFT, Molecular docking, 4PYP, HepG-2, ADMET.**

---

1. INTRODUCTION

Plants have been a vital source of medicinal substances for thousands of years, with many contemporary remedies derived from natural origins. The importance of plants in drug discovery can be seen in several areas.[1] Plants have been used in traditional medicine for centuries, with ancient civilizations such as the Egyptians and Chinese documenting their use. The Ebers Papyrus, an ancient Egyptian medical manuscript, contains over 700 herbal remedies.Plants have inspired the design, discovery, and development of new drugs[2]. Many plant-derived natural products have been commercialized as pharmaceutical medications, such as Paclitaxel derived from *Taxus brevifolia*, used to treat lung, ovarian, and breast cancer[3]. Artemisinin derived from *Artemisia annua*, used to treat malaria. Silymarin derived from *Silybum marianum*, used to treat hepatic disorders. Digitoxin derived from the foxglove plant, used to manage cardiac ailments[4].

Plant-based pharmaceutical techniques offer an efficient, cost-effective, and safe alternative to conventional procedures. Plant-made pharmaceuticals can provide patients with greater and quicker access to medications[5].The continuous exploration of global biodiversity and the development of new technologies will likely lead to the discovery of more plant-derived natural products with therapeutic potential[6]. Researchers are working to standardize herbal remedies and identify analytical marker biomolecules to support future drug discoveries.Some notable benefits of plant-derived natural products include, plants offer a vast array of structural diversity, which can lead to the discovery of new medications. Plant-derived natural products have shown promise in treating various diseases, including cancer, malaria, and cardiac ailments[7]. Plant-based pharmaceuticals can be more cost-effective than traditional

methods.Overall, plants continue to play a significant role in drug discovery and development, offering a wealth of opportunities for future research and innovation[8].

Density Functional Theory (DFT) is a computational method that has become increasingly important in drug discovery, particularly in the study of isolated compounds from plants[9]. DFT provides a powerful tool for understanding the electronic structure and properties of molecules, which is crucial in designing and optimizing lead compounds. DFT calculations can predict various molecular properties, such as energy levels, molecular orbitals, and electrostatic potential, which are essential in understanding the reactivity and interactions of molecules[10]. DFT studies can help establish SARs (Structure-Activity Relationship) by analyzing the electronic structure and properties of molecules and their biological activity[11]. DFT calculations can be used to predict the binding affinity and orientation of molecules to target proteins, which is critical in drug design.DFT studies can predict ADME (Absorption, Distribution, Metabolism, and Excretion) properties, such as solubility, permeability, and metabolism, which are essential in drug development[12]. DFT calculations can be performed computationally, reducing the need for expensive experimental methods. DFT studies can provide rapid insights into molecular properties and behavior, accelerating the drug discovery process. DFT calculations can provide accurate predictions of molecular properties and behavior, guiding experimental design and optimization[13]. DFT studies play a vital role in drug discovery, particularly in the study of isolated compounds from plants. By providing insights into molecular properties and behavior, DFT calculations can help optimize lead compounds and accelerate the drug discovery process[14].

The leaves of *Coccinia grandis (L.)*, sometimes referred to as ivy gourd leaves, are used in traditional medicine to treat a number of conditions, such as burns, pneumonia, jaundice, and skin eruptions[15]. They are also thought to have wound-healing, antioxidant, and antidiabetic qualities. The leaves' therapeutic qualities are a result of the vitamins, minerals, and phytochemicals they contain Beta-carotene and flavonoids, which have antioxidant properties, are found in *Coccinia grandis (L.)* leaves[16]. According to research, *Coccinia grandis (L.)* can lower blood sugar levels by boosting insulin synthesis and blocking enzymes involved in glucose metabolism[17]. *Coccinia grandis (L.)* extract has been shown in studies to facilitate wound healing in vitro.The bioactive components in the plant may help shield the kidneys from diabetic kidney damage[18]. Extracts from *Coccinia grandis (L.)* have been shown in several investigations to possess antibacterial properties against specific bacteria[19]. It's important to speak with a healthcare provider before utilising *Coccinia grandis (L.)* for medical purposes, even if it has showed promise in both traditional and scientific investigations[20]. To completely comprehend its effects and possible negative effects, more research is required.Qualified medical professionals should decide whether the plant is safe and effective for a certain ailment[21]. The present work involved the isolation and identification of natural components from the seed of *Coccinia grandis (L.)* methanolic extract. *Coccinia grandis (L.*) has yielded four newly identified bioactive compounds. Compound 1, which was a steroid, was selected for additional in vitro and in silico study because of its similarity to cholesterol. Numerous biological actions for a range of human illnesses and conditions may be present in these natural substances. These bioactive substances may prove to be a valuable source for new drug development in the future and guarantee therapeutic necessity.

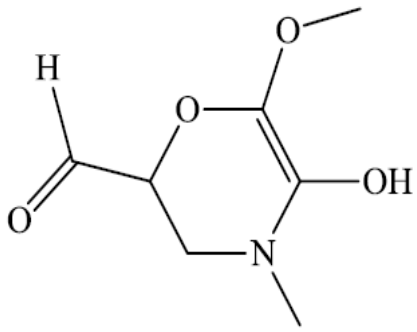

Compound - 1

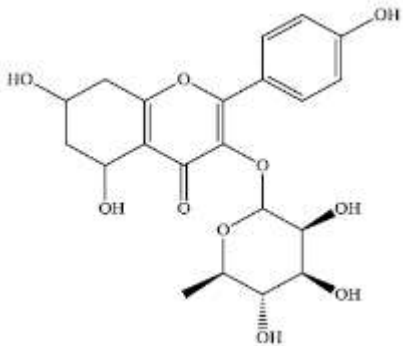

Compound - 2

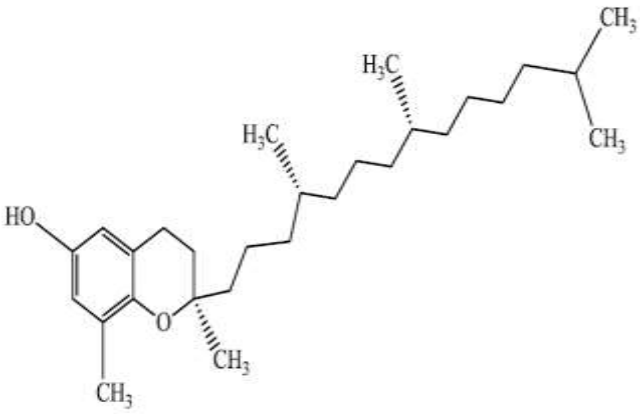

Compoud-3

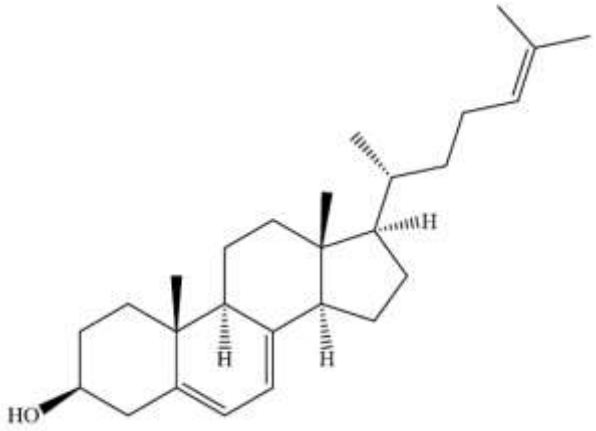

Compound-4

The only secondary metabolites on Earth with the ability to absorb UV rays are the bioactive chemicals found in abundance in Coccinia grandis (L.) leaves. Therefore, methanolic extract that is high in flavonoids, alkaloids, and lipids can be utilised safely to prepare clinical medications, make antioxidant herbal drinks, and even produce anti-cancer chemicals by bioactivity-guided fractionation. Using flash column chromatography, four chemicals were extracted from Coccinia grandis (L.). These four compounds were the first isolated reports from Coccinia grandis (L.) and were identified by spectroscopic data. The majority of the chemicals can be used to treat a variety of illnesses. The purpose of this research is to identify novel plant potentials as therapeutic targets.

A research paper that focusses on the isolation, characterisation, and DFT study of a bioactive compound from a plant extract would include several important steps: first, the bioactive compound would have to be extracted from the plant material using techniques like solvent extraction or maceration; next, the extract would be subjected to different separation techniques (chromatography, etc.) to isolate the target compound; after that, the structure of the compound would be characterised using techniques like spectroscopy (IR, NMR); and lastly, a DFT study would be conducted to discover the electronic structure and properties of the compound, which could reveal information about its bioactivity[22].The conventional oral dosages of cefdinir for treatment of lung infectious diseases have multiple drawbacks such as orally given drugs cannot provide sufficient amount of drug for the lung site that requires increased amounts of dose due to this there is a need to have dosage such as DPI[23]. In this research, the functioned MWCNTs were loaded with cefdinir drug which has efficient treatment against CF lung infections, which is evaluated by particle size, flow properties, release kinetics, in vitro, and in vivo deposition study, and acute inhalation toxicity study. Applications of density functional theory (DFT) to explain a wide range of issues of pharmaceutical and biological interest have been becoming more and more popular. Due to their usage in determining the reactivity and bioactivity of compounds utilised in biomedical applications, dipole moment and global characteristics are of great interest[24].

2. MATERIALS AND METHODS:

2.1 Preparation of plant extracts:

To extract chemicals with a wide range of polarity, the plant extracts were made using a serial exhaustive extraction approach. First, 500 grammes of the powdered samples were put in a stoppered container with hexane as the solvent. They were then let to stand at room temperature for 21 days (72 hours) while being constantly stirred to dissolve the soluble material. Following that, Whatman No. 1 filter paper was used to filter the extract. After being air dried, the remaining marc was extracted once more using the solvent ethyl acetate for a further 21 days. Methanol extraction was the next step. A separate aqueous extract was made by extracting the dry ground sample with water.

2.2 TLC Profile:

The crude extracts of *Wrightia tinctoria* R.Br. *Physalis minima* Linn., *Diplocyclos palmatus* (L.) Jeffery were subjected to TLC in solvents of different polarity range at different ratios. Each of the four extracts were run in eight different solvent systems viz., PE: EA= 9:1, PE: EA=8.5 :1.5, PE: EA= 8:2, PE: EA = 7.5: 2.5, PE: EA= 6.5: 3.5, PE: EA: M = 9: 0.5: 0.5, PE: EA: M = 8: 1.5: 0.5, PE: EA: M = 7.5: 1.5: 1 on analytical plates over Silica gel (TLC grade, Merck India).

2.3 Column Chromatography:

Using petroleum ether as a solvent, 500g of silica gel (4×100cm) was used for column chromatography in order to separate the constituents of the plant crude extract. Before being used, the column was thoroughly dried and cleaned with petroleum ether. Over the silica gel, 10g of an ethanolic stem extract of Coccinia grandis (L.) seeds was applied. Solvents such as petroleum ether, chloroform, ethyl acetate, ethanol, and water were then used one after the other to elute the column. For additional analysis, the column fractions were gathered in 20 ml test tubes.

2.4 Characterization:

Melting points in capillaries made of open glass were not noted. Using an ATR Bruker alpha FT-IR spectrophotometer (R. C. Patel College, Shirpur, India), the IR and UV-visible spectra were captured on a Shimadzu. Thermo Finnigan, calibrated using the K-factor method (Punjab University, Chandigarh, India), performed NCHS analyses; a Brucker spectrophotometer (SSPU Pune, India) recorded 13C and 1H NMR spectra at 500.13 MHz; and Wockhart R & D Lab, Aurangabad, India, Single Crystal Instrument, verified the LC-MS. Model: University of Hyderabad, India; X-ray wavelength: Mo; x-cen: 390.4189; y-cen: 185.8663; distance: 51.0000; beam: -0.0435 (Model Interpol. in use). The reference books and table charts on the Sigma-Aldrich website were expected to provide the interpretation of all the separated compounds' spectrum data.

2.5 Computational Methods

The quantum computational studies for the examined compounds **1** to **4** were carried out in the gas phase using the ORCA program package (version 4.0.1). The atomic co-ordinates of all compounds were building using the Avogadro software[25], and then further processed to generate the ORCA input file for the geometry optimization calculations. The DFT- B3LYP method with 6–311G(d,p) and 6-311+G(d,p) basis set were used for all the geometry optimizations and energy calculations[26,27,28,29].

3. **RESULT**

3.1 Spectral Data of Isolated Compounds

3.1.1 Compound - 1

3.1.1.1 UV-Visible: The UV-Visible spectroscopy analysis for compound-1 Figure 3.4 (B) showed the major absorption bands at 263nm and maximum absorbance at 3.248

3.1.1.2 FTIR (Fourier Transformation Infrared) cm^{-1}: C=C Stretching: 1628.40 cm^{-1} – 1604-41 cm^{-1}; C=C bending: 937.40 cm^{-1}; –C–N Aromatic amine: 1235.53 cm^{-1}; –CH_3 group: 1445.22 cm^{-1} ; C=O carbonyl group: 1734.52 cm^{-1}; –CHO group: 2984.74 cm^{-1}; –OH group: 3377.61 cm^{-1}; –OH alcohol bending: 1372.28 cm^{-1}; Aromatic group: 1500.54 cm^{-1} ; C–O–C ether group: 1043.12 $cm^{-1.}$

3.1.1.3 The exhibiting signals at ^{1}HNMR (500.13 MHz; DMSO d6) δ ppm: 7.00 (s, 1H, –CHO); 4.05 - 4.00 (s, 1H, –OH); 3.32–2.52 (s, 3H, –OCH_3); 2.51 – 2.49 (s, 3H, –CH_3); 2.08 – 1.98 (t, 3H, –CH); 1.18-1.16 (d, 2H, cyclic –CH.

3.1.1.4 ^{13}CNMR (500.13 MHz; DMSO d^{6}) ppm: 14.55 (methyl carbon); 114.32 – 116.25 (ring C=C); 60.22 (C–O–CH_3); 21.22–40.57 (carbonyl carbon); 170.81 (carboxylic ester); 39.48–31.15 (cyclic N–CH_3); 40.57–40.48 (cyclic –CH_2); 129.25 (cyclic ethylene).

3.1.2Compound -2

3.1.2.1 UV-Visible: Major absorption bands at λmax of 252nm and at maximum absorbance is 1.77

3.1.2.2 FTIR (Fourier Transformation Infrared) cm^{-1}: Aliphatic / Aromatic ester: 1215.88 cm^{-1}; –CH_3 group: 1377.78 cm^{-1}; C=O carbonyl group: 1638.52 cm^{-1}; –OH group: 3312.84 cm^{-1}; Aromatic group: 1480.72 cm^{-1}; C–O–C ether group: 1109.31 $cm^{-1.}$

3.1.2.3 ^{1}HNMR (500.13 MHz; DMSO d6) δ ppm: 8.31 (dd, 4H, Ar); 3.40–3.31 (s, 6H, – OH); 1.10 (s, 3H, –CH_3–); 2.50 (t, 5H, –CH–); 2.49 (p, 5H, –CH), 1.10 -1.07 (d, 1H, cyclic –CH–).

3.1.2.4 ^{13}CNMR (500.13 MHz; DMSO d6) ppm: 15.63 (methyl carbon); 65.38 (C–O–C); 39.48 (carbonyl carbon); 40.24 – 40.07 (cyclic –CH_2–); 79.64 (cyclic –CH–).

3.1.3 Compound -3

3.1.3.1 UV-Visible: Major absorption bands at λ_{max} of 252nm and at maximum absorbance is 1.777.

3.1.3.2 FTIR (Fourier Transformation Infrared) cm^{-1}: Aromatic ether: 1270.66 cm^{-1}; – CH_3 group: 1379.85 cm-1 - 1326.66 cm^{-1}; –OH group: 3329.45 cm^{-1}; –CH bending overtone (weak): 2008.07 cm^{-1} –1921.75 cm^{-1}; Aromatic group: 1498.54 cm^{-1} -1450.20 cm^{-1}; C–O–C group: 1174.38 cm^{-1}; –CH bending: 879.71 cm^{-1}.

3.1.3.3 ^{1}HNMR (500.13 MHz; DMSO d6) δ ppm: 7.00–6.99 (s, 2H, Ar); 4.97–4.33 (s, 3H, –OH); 1.98 (s, 6H, $–CH_3$); 2.50–2.49 (d, 12H, $–CH_3$); 3.46 (m, 1H, terminal –CH–); 2.49 (p, 2H, –CH), 2.50 (t, 4H, cyclic $–CH_2–$); 3.16 (t, 1H, chain $–CH_2–$); 2.50 (p, 15H, chain $–CH_2–$)

3.1.3.4 ^{13}CNMR (500.13 MHz; DMSO d^6) ppm: 19.01 (methyl carbon); 56.49 (C–O–C); 40.07 – 40.57 (cyclic $–CH_2–$); 49.06 (cyclic –CH–); 114.31 – 116.08 (ring C=C); 129.25 – 149.05 (Carbon in aromatic rings)

3.1.4 Compound -4

3.1.4.1 UV-Visible: Major absorption bands at λ_{max} of 252nm and at maximum absorbance is 1.777

3.1.4.2 FTIR (Fourier Transformation Infrared) cm^{-1}: C=C Stretching: 1635.73 cm^{-1}; C=C bending: 1015.51 cm-^{1}; –OH group: 3269.14 cm^{-1}; –CH bending overtone (weak): 2038.24 cm^{-1}.

3.1.4.3 ^{1}HNMR (500.13 MHz; DMSO d^6) δ ppm: 8.31 (dd, 2H, Ar); 4.03–4.00 (s, 1H, –OH); 1.18–1.16 (s, 12H, $–CH_3$); 1.98 (q, 4H, $–CH_2–$); 2.49–2.08 (d, 3H, –CH–); 2.50 (t, 12H, $–CH_2–$), 3.32 (m, 6H, $CH_3–C–CH_2–$); 2.49 (t, 2H, –CH–)

3.1.4.4 ^{13}CNMR (500.13 MHz; DMSO d^6) ppm: 14.43 (methyl carbon); 40.55–40.05 (cyclic $–CH_2$); 39.96–31.42 (cyclic –CH–)

3.2 DFT Calculations Studies

Table 1: Thermal parameter and dipole moment (Debye) of compound **1**, **2**, **3** and **4**

Parameters	1	2	3	4
E_{Tot}	-628.7692	-1566.3809	-1245.8396	-1128.8276
Total Dipole Moment	2.25475	7.66962	2.98433	1.21705

E_{Tot}: Sum of electronic and thermal energies

3.3 Frontier Molecular Orbitals

Frontier molecular orbitals (FMOs) are the highest occupied molecular orbital (HOMO) and lowest unoccupied molecular orbital (LUMO). Usually, in FMOs the HOMO is acts as an electron donor, while, the LUMO is acting as an electron acceptor and they have been used for the study of several important quantum chemical parameters such as chemical reactivity, aromaticity, conjugation and lone pair. The FMOs can control the binding mode of the drugs with other receptor molecules and gives accurate qualitative information about the probability of the electrons to transfer from the HOMO to the LUMO. Recently, numerous scientific studies showed that there is a correlation between FMOs of the drug molecules for the study of several biological activities such as anticancer[30,31], antifungal[32], antimicrobial [33] and cytotoxic activities[34] which can be useful in the new drug-design field[35].

3.4 Chemical Reactivity Descriptors

Table 2: Calculated electronegativity (χ), global hardness (η), softness (δ), global electrophilicity index (ω), the ionization potential (I) and the electron affinity (A) (in eV) of investigated compound **1**, **2**, **3** and **4**

Compound	1	2	3	4
E_{HOMO}	-3.8938	-5.9084	-5.1453	-5.2217
E_{LUMO}	-1.3811	-1.6587	-0.0337	-0.4102
ΔE	2.5127	4.2497	5.1116	4.8115
χ	2.6374	3.7835	2.5895	2.8159
η	1.2563	2.1248	2.5558	2.4057
δ	0.7959	0.4706	0.3912	0.4156
ω	2.7683	3.3685	1.3118	1.6480
I	3.8938	5.9084	5.1453	5.2217
A	1.3811	1.6587	0.0337	0.4102

Fig 1A: Optimized geometry of compound **1** obtained at the B3LYP/ 6-311G(d,p)

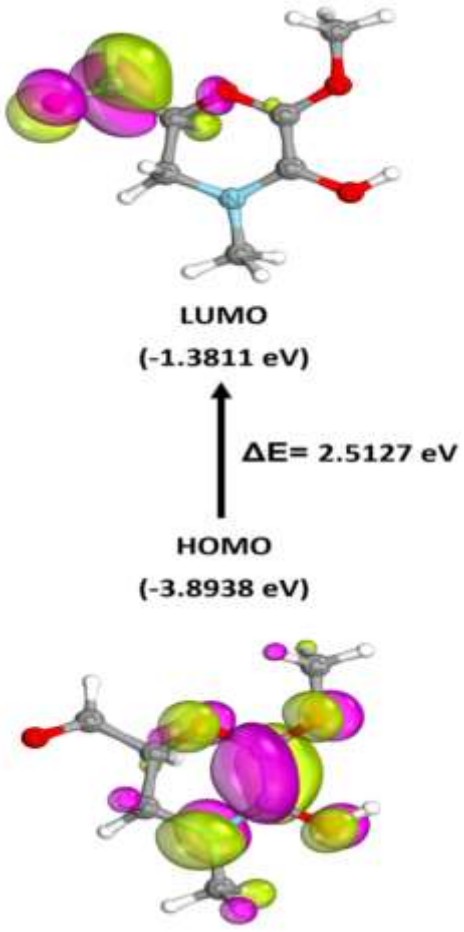

.

Figure 1B: FMOs of compound **1**.

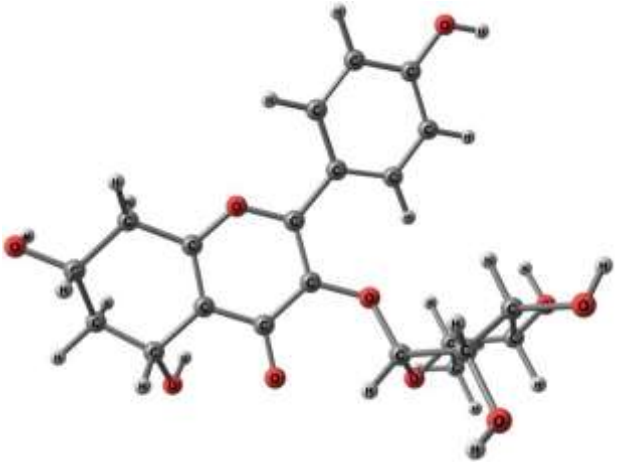

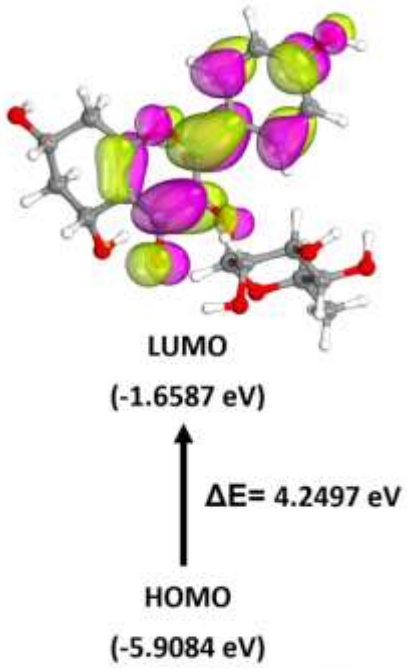

Fig 2A: Optimized geometry of compound **2** obtained at the B3LYP/ 6-311G(d,p).

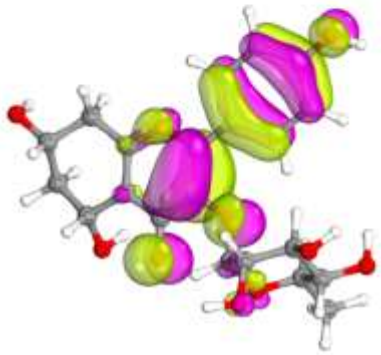

Figure 2B: FMOs of compound **2**.

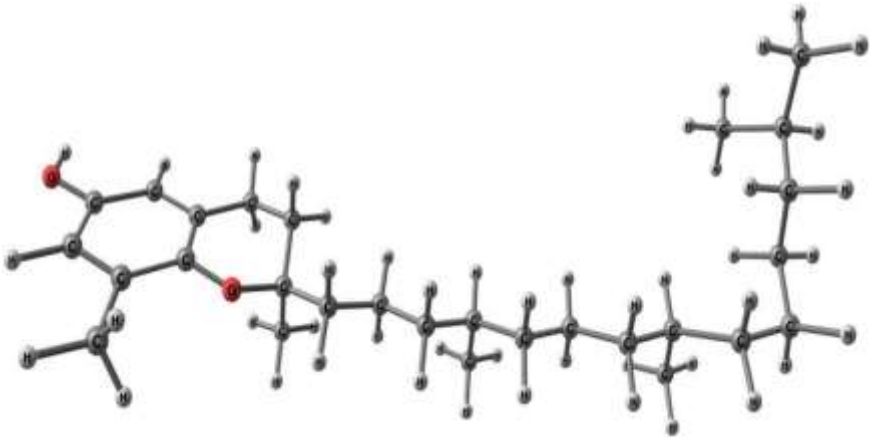

Fig 3A: Optimized geometry of compound **3** obtained at the B3LYP/ 6-311G(d,p).

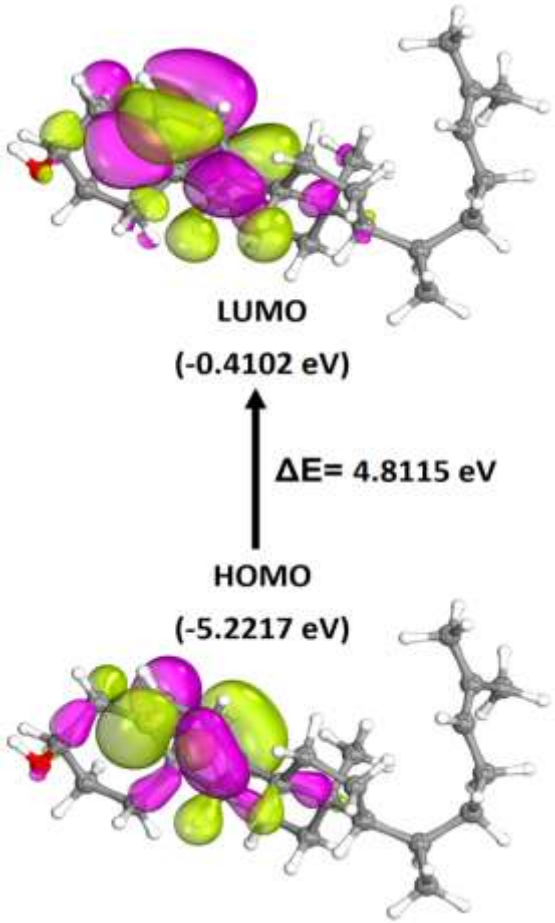

Figure 3B: FMOs of compound **3**.

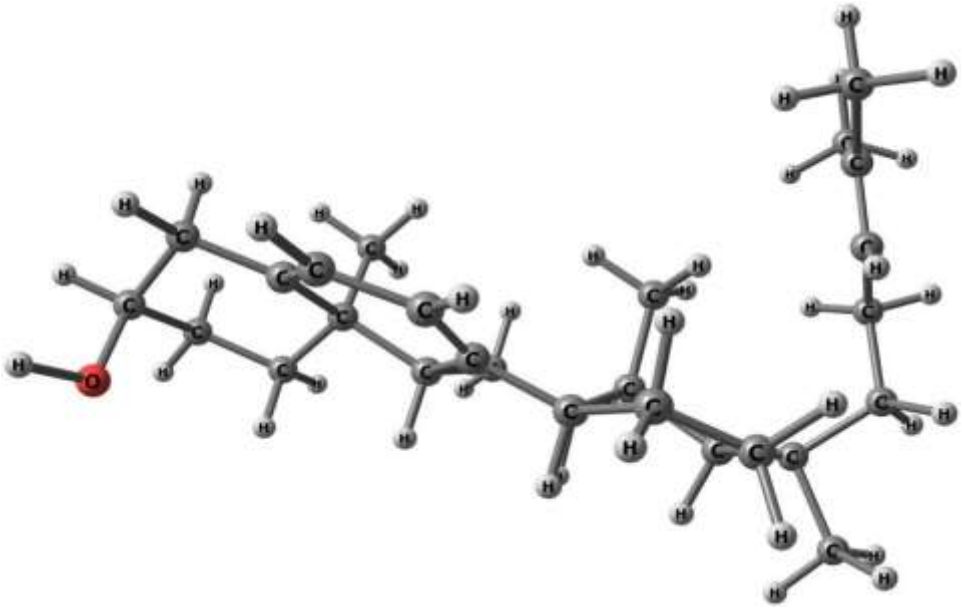

Fig 4A: Optimized geometry of compound **4** obtained at the B3LYP/ 6-311G(d,p)

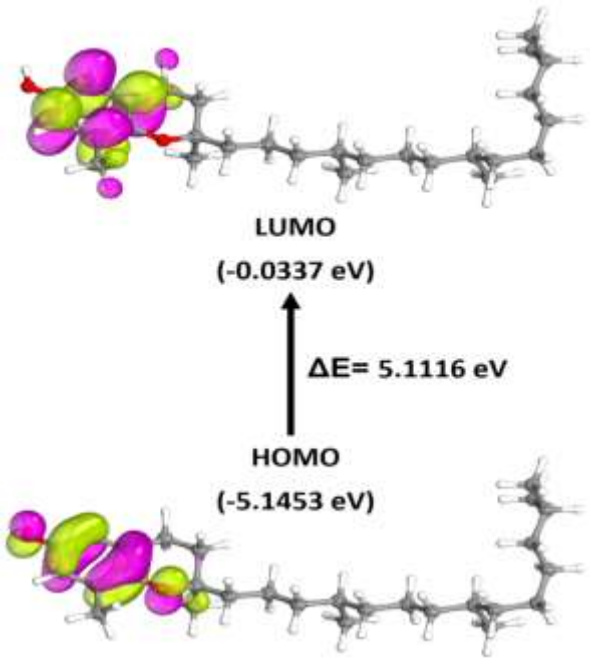

Figure 4B: FMOs of compound **4**.

3.5 CARTESIAN COORDINATES OF ALL THE COMPOUNDS:

CARTESIAN COORDINATES (ANGSTROEM)

Table 3: Atomic Cartesian coordinates for all 6-31G** optimized compounds

Compoud 1

C	1.081	-0.160	-0.090
N	2.333	-0.321	0.655
C	3.084	0.899	0.904
C	4.121	1.136	-0.219
O	5.052	0.060	-0.249
C	4.445	-1.175	-0.140
O	5.251	-2.223	-0.462
C	6.393	-2.394	0.397
C	3.167	-1.361	0.237
O	2.580	-2.600	0.268
C	4.912	2.414	-0.038
O	4.391	3.491	0.104
H	0.394	0.460	0.487
H	0.629	-1.140	-0.232
H	1.232	0.301	-1.080
H	3.618	0.809	1.855
H	2.409	1.752	0.964
H	3.586	1.189	-1.181
H	6.913	-3.283	0.042
H	6.074	-2.536	1.435
H	7.056	-1.528	0.330
H	3.195	-3.208	-0.160
H	6.014	2.278	-0.038

Compound 2

O	1.801	2.112	0.973		H	1.979	2.866	1.508
C	0.512	2.105	0.578		C	3.837	3.604	2.249
C	0.108	0.919	0.171		C	2.968	3.408	0.165
C	1.445	0.925	0.236		H	0.471	4.246	3.633
C	2.200	2.118	0.240		O	3.927	1.676	0.030
C	1.548	3.306	0.159		C	1.283	2.348	2.968
C	0.212	3.297	0.568		H	1.018	1.518	2.278
C	3.635	2.199	0.674		O	2.507	2.912	2.572
O	4.083	3.418	0.966		C	1.416	1.759	4.377
C	5.307	3.692	1.389		H	2.159	0.927	4.347
C	5.662	5.139	1.615		O	1.873	2.760	5.253
C	7.181	5.369	1.731		H	2.338	1.306	0.992
O	7.452	6.694	2.112		H	0.448	.161	0.011
C	7.783	4.369	2.710		H	0.010	0.569	1.848
C	7.622	2.935	2.164		H	2.073	4.253	0.167
O	7.965	2.025	3.179		H	0.261	4.221	0.876
C	6.228	2.652	1.601		H	5.123	5.475	2.527
C	5.835	1.345	1.263		H	5.306	5.750	0.757
O	6.626	0.433	1.427		H	7.657	5.196	0.740
C	4.528	1.094	0.770		H	7.072	6.832	3.019
O	0.149	0.389	0.168		H	7.250	4.475	3.682
C	1.241	0.042	0.886		H	8.863	4.569	2.882
O	2.279	4.847	0.929		H	8.327	2.780	1.318
C	2.788	3.536	1.139		H	7.259	2.074	3.877
H	3.176	4.007	3.377		H	0.322	3.178	1.092
H	1.950	4.270	4.675		H	2.495	2.963	1.581
H	2.471	4.240	2.593		H	2.2640	6.041	2.3

Compound 3

C	2.981	0.422	.775	H	1.720	2.820	0.521
C	2.690	1.021	1.209	H	1.034	1.345	0.133
C	1.867	1.038	2.505	H	3.797	2.436	0.888
C	1.985	1.837	0.108	H	2.989	1.093	1.665
C	2.808	2.053	1.169	H	2.059	4.011	1.671
C	2.179	3.040	2.168	H	2.888	3.213	2.984
C	0.813	2.633	2.750	H	0.079	2.579	1.937
C	0.763	1.309	3.541	H	0.466	3.442	3.408
H	1.099	0.501	2.877	H	2.733	1.524	4.474
C	1.696	1.337	4.761	H	1.679	0.390	5.306
C	0.694	0.996	3.937	H	1.396	2.129	5.458
C	0.934	0.398	4.531	H	1.326	1.107	3.046
C	2.418	0.673	4.813	H	1.041	1.758	4.649
C	2.747	2.096	5.310	H	0.356	0.510	5.453
H	2.324	2.805	4.583	H	0.554	1.157	3.833
C	2.114	2.386	6.680	H	2.986	0.488	3.893
C	4.275	2.307	5.326	H	2.789	0.054	5.548
C	4.738	3.749	5.583	H	1.028	2.270	6.656
C	6.263	3.888	5.481	H	2.320	3.406	7.014
C	6.841	5.294	5.716	H	2.506	1.700	7.439
C	6.522	5.819	7.123	H	4.681	1.980	4.361
C	6.426	6.280	4.612	H	4.719	1.644	6.081
C	7.169	7.613	4.734	H	4.405	4.073	6.574
C	8.645	7.395	4.978	H	4.249	4.410	4.858
C	9.572	8.425	4.770	H	6.598	3.558	4.491
C	10.92	8.216	4.989	H	.740	3.218	6.205
O	11.87	9.191	4.799	H	5.462	6.065	7.223
C	11.37	6.963	5.418	H	7.101	6.718	7.348
C	10.47	5.923	5.637	H	6.775	5.063	7.870
C	10.94	4.566	6.097	H	5.345	6.443	4.646
C	9.105	6.152	5.417	H	6.655	5.818	3.646
O	8.277	5.074	5.631	H	6.741	8.210	5.549
H	3.472	0.981	1.577	H	7.027	8.202	3.822
H	2.051	0.947	0.527	H	9.218	9.394	4.425
H	3.632	0.466	0.101	H	10.67	3.791	5.372
H	3.653	1.417		H	10.46	4.285	7.041
H	0.891	0.564	2.354	H	1.690	2.060	2.852
H	2.377	0.495	3.307				

Compound 4

C	2.128	2.471	1.277	C	1.082	0.078	1.231
C	2.033	1.348	0.277	H	2.185	3.461	0.780
C	2.022	1.660	1.2	H	3.038	2.342	1.901
C	1.954	0.079	0.733	H	1.233	2.466	1.936
C	1.864	1.118	0.176	H	2.092	2.751	1.388
C	1.806	2.460	0.568	H	1.079	1.294	1.657
C	0.434	3.099	0.983	H	2.886	1.171	1.698
H	0.195	3.205	0.072	H	1.969	0.084	1.804
C	0.775	4.546	1.424	H	2.818	1.099	0.749
C	0.475	2.456	2.098	H	1.034	1.062	0.910
H	1.122	3.316	2.397	H	2.533	2.461	1.410
C	0.188	2.033	3.434	H	2.211	3.171	0.188
C	0.812	1.049	4.094	H	1.324	5.091	0.627
C	2.099	1.230	3.284	H	0.145	5.137	1.624
H	2.530	2.203	3.626	H	1.401	4.541	2.343
C	3.256	0.257	3.378	H	1.160	1.517	3.318
C	3.3	4.322	0.692	H	0.349	2.947	4.047
C	4.509	4.548	1.493	H	0.446	0.016	3.922
C	5.574	3.732	1.435	H	0.912	1.172	5.194
C	6.778	4.012	2.321	H	2.472	5.8	0.833
C	8.061	3.998	1.477	H	4.514	5.405	2.160
H	8.949	4.108	2.142	H	6.861	3.222	3.095
O	8.045	5.048	0.543	H	6.685	4.977	2.864
C	8.182	2.648	0.740	H	8.240	5.882	1.047
C	6.970	0.185	2.417	H	8.264	1.824	1.479
C	5.597	2.475	0.557	H	9.113	2.641	0.133
C	5.464	1.274	1.537	H	7.080	1.451	1.538
C	4.447	0.552	2.467	H	7.003	0.948	3.226
H	4.836	1.481	2.940	H	6.238	1.264	2.327
C	3.990	0.969	1.023	H	5.584	0.305	1.012
C	2.8	1.955	1.007	H	4.475	1.3	2.043
C	1.6	1.405	1.838	H	3.662	0.086	0.448

3.6 DISCUSSION

3.6.1 DFT Calculations Studies

The geometrical optimization of compounds **1**, **2**, **3** and **4** were done in the gas phase using theoretical DFT calculations to get the minimized energy molecular compound and frequencies of the optimized molecular compound by which different thermochemical parameters are also calculated. **Figure 1A**, **2A**, **3A** and **4A** shows the optimized molecular compounds of investigated compound (**1** to **4**) which shows non-planarity for both compounds and are stable as a consequence of the absence of the imaginary frequency. The DFT calculated results for thermal parameters and dipole moment of the compound **1** to **4** are summarized in **Table 1**. From the results, it was observed that the dipole moment of compounds **1**, **2**, **3** and **4** is 2.25475, 7.66962, 2.98433 and 1.21705 Debye in the gas phase respectively. The high dipole moment value of compound **2** ensures there is a strong intramolecular interaction and hence the compound **2** influences their active binding pose towards a specific target protein [31].

The frontier molecular orbitals of investigated compounds **1**, **2**, **3** and **4** to compare the energy level of the HOMO and LUMO along with their energy gap were calculated using the DFT B3LYP/6–311+G(d,p) method and are presented in **Table 2**. **Figure 1B**, **2B**, **3B** and **4B** shows the calculated 3D isodensity surface plots for FOMs of investigated compounds **1** to **4**. The energy levels of HOMOs of the compound **1** to **4** under investigation are -3.8938, -5.9084, -5.1453 and -5.2217 eV respectively, while, the LUMOs are -1.3811, -1.6587, -0.0337 and -0.4102 eV respectively subject to the degree of conjugation as well as the atmosphere of the attached substituents around the nucleus. Likewise, the energy gap for compounds **1** to **4** was ΔE = 2.5127, 4.2497, 5.1116 and 4.8115 eV, respectively. From these results it is clear that the compound **2** has the high lying HOMO, E_{HOMO} = -5.9084 eV, is susceptible to be a good electron donor, while E_{LUMO} = -1.6587 eV, is considered to be the best electron acceptor and hence this data could confirm that, compound **2** has higher binding affinity as compared to compounds **1**, **3** and **4**. Moreover, compound **2** with moderate energy gap

ΔE = 4.2497 eV in comparison to other compounds validates the highest binding affinity which can enable binding of the drug molecules with the receptors[36].

To further explore the chemical reactivity of investigated compounds **1**, **2**, **3** and **4**; the frontier molecular orbitals of compounds **1**, **2**, **3** and **4** are used to estimate other chemical reactivity descriptors along with ionization potential ($I= -E_{HOMO}$) and the electron affinity ($A = -E_{LUMO}$) such as electronegativity (χ), global hardness (η), softness (δ) and electrophilicity (ω)[37]. The obtained results are shown in **Table 2**.

From **Table 3**, it is observed that compound **2** has higher basicity (χ = 3.7835 eV) as compared to compounds **1**, **3** and **4** which could be another aspect for its higher binding affinity. Similarly, the global hardness for compound **2**, **3** and **4** from the gas phase is significantly high (2.1248, 2.5558 and 2.4057 eV), which confirm compounds **2**, **3** and **4** are chemically stable. Moreover, the moderate electrophilicity index of compound **2** (ω = 3.3685 eV) confirms the strong energy transformations in the FMOs of **2**[38]. All these aspects could share together with different extent to considerably influence the degree of the binding affinity of these compounds with active protein sites.

3.7 Conclusion:

The purpose of this study was to isolate eight bioactive compounds (numbers 1–4) from *Coccinia grandis L*. leaves for the first time. Various pectroscopic methods were applied to the characterisation process.The dipole moment of compounds 1, 2, 3, and 4 was found to be 2.25475, 7.66962, 2.98433, and 1.21705 Debye in the gas phase, respectively, based on DFT. Compound 2 influences their active binding pose towards a particular target protein because of its high dipole moment value, which guarantees a strong intramolecular interaction.The data may confirm that compound 2 has a higher binding affinity than compounds 1, 3, and 4 because the frontier molecular orbitals of the investigated results clearly show that compound 2 has a high lying HOMO, EHOMO = -5.9084 eV, which makes it susceptible to be a good electron donor, while ELUMO = -1.6587 eV, which is thought to be the best electron acceptor. Furthermore, compared to other compounds, compound 2's mild energy gap (ΔE = 4.2497 eV) confirms the highest binding affinity, allowing medication molecules to bind to receptors.The chemical stability of compounds 2, 3, and 4 is further supported by their notably high global hardness values from the gas phase (2.1248, 2.5558, and 2.4057 eV). Furthermore, the substantial energy changes in compound 2's FMOs are confirmed by its moderate electrophilicity index (ω = 3.3685 eV). To varying degrees, all of these factors may work together to significantly affect how well these substances bind to active protein locations.

CONFLICT OF INTEREST

The authors have no conflicts of interest regarding this investigation**.**

ACKNOWLEDGMENTS

The authors remain grateful to Dr. V. R. Patil, Principle, Rani Laxmibai Mahavidyalay Parola, Jalgaon for their consistent encouragement and support during this work.

REFERENCES

1. Chaachouay N, Zidane L. Plant-derived natural products: a source for drug discovery and development. Drugs and Drug Candidates. 2024 Feb 19;3(1):184-207.
2. Heyn B. Ayurveda: The Indian art of natural medicine and life extension. Inner Traditions/Bear & Co; 1990.
3. Sati P, Sharma E, Dhyani P, Attri DC, Rana R, Kiyekbayeva L, Büsselberg D, Samuel SM, Sharifi-Rad J. Paclitaxel and its semi-synthetic derivatives: comprehensive insights into chemical structure, mechanisms of action, and anticancer properties. European journal of medical research. 2024 Jan 30;29(1):90.
4. CHEEMA HS. MEDICINAL PLANTS AS A SOURCE OF ANTIMALARIAL COMPOUNDS: COUNTERING THE THREAT OF DRUG RESISTANCE. Phytomolecules as a Source for Drug Discovery: Antimicrobials from Medicinal Plants. 2025 Apr 2:25.
5. Nasim N, Sandeep IS, Mohanty S. Plant-derived natural products for drug discovery: Current approaches and prospects. The Nucleus. 2022 Dec;65(3):399-411.
6. Aware CB, Patil DN, Suryawanshi SS, Mali PR, Rane MR, Gurav RG, Jadhav JP. Natural bioactive products as promising therapeutics: A review of natural product-based drug development. South African Journal of Botany. 2022 Dec 1;151:512-28.

7. Dehelean CA, Marcovici I, Soica C, Mioc M, Coricovac D, Iurciuc S, Cretu OM, Pinzaru I. Plant-derived anticancer compounds as new perspectives in drug discovery and alternative therapy. Molecules. 2021 Feb 19;26(4):1109.
8. Haider MW, Abbas SM, Saeed MA, Farooq U, Waseem M, Adil M, Javed MR, Haq IU, Osei Tutu C. Environmental and Nutritional Value of Fruit and Vegetable Peels as Animal Feed: A Comprehensive Review. Animal Research and One Health. 2025.
9. Ahmad I, Jagatap V, Patel H. Application of density functional theory (DFT) and response surface methodology (RSM) in drug discovery. InPhytochemistry, computational tools and databases in drug discovery 2023 Jan 1 (pp. 371-392). Elsevier.
10. Suresh CH, Remya GS, Anjalikrishna PK. Molecular electrostatic potential analysis: A powerful tool to interpret and predict chemical reactivity. Wiley Interdisciplinary Reviews: Computational Molecular Science. 2022 Sep;12(5):e1601.
11. Noureddine O, Issaoui N, Medimagh M, Al-Dossary O, Marouani H. Quantum chemical studies on molecular structure, AIM, ELF, RDG and antiviral activities of hybrid hydroxychloroquine in the treatment of COVID-19: Molecular docking and DFT calculations. Journal of King Saud University-Science. 2021 Mar 1;33(2):101334.
12. Sucharitha P, Reddy KR, Satyanarayana SV, Garg T. Absorption, distribution, metabolism, excretion, and toxicity assessment of drugs using computational tools. InComputational approaches for novel therapeutic and diagnostic designing to mitigate SARS-CoV-2 infection 2022 Jan 1 (pp. 335-355). Academic Press.
13. Gallegos LC, Luchini G, St. John PC, Kim S, Paton RS. Importance of engineered and learned molecular representations in predicting organic reactivity, selectivity, and chemical properties. Accounts of Chemical Research. 2021 Feb 3;54(4):827-36.
14. Jorgensen WL. Efficient drug lead discovery and optimization. Accounts of chemical research. 2009 Jun 16;42(6):724-33.
15. Beera AM, Nori LP, Seethamraju SM. Nutritional and therapeutic potential of Coccinia grandis (L) Vogit: a wonder vegetable. Pharma Times. 2022 Jul;54(07):7.
16. Sarkar T, Salauddin M, Roy S, Chakraborty R, Rebezov M, Shariati MA, Thiruvengadam M, Rengasamy KR. Underutilized green leafy vegetables: frontier in fortified food development and nutrition. Critical Reviews in Food Science and Nutrition. 2023 Dec 20;63(33):11679-733.
17. Meenatchi P, Purushothaman A, Maneemegalai S. Antioxidant, antiglycation and insulinotrophic properties of Coccinia grandis (L.) in vitro: Possible role in prevention of diabetic complications. Journal of traditional and complementary medicine. 2017 Jan 1;7(1):54-64.
18. Singh JK, Chakraborty S, Nagpal M, Aggarwal G. Herbal approach for diabetic cure and futuristic dimension. Current Drug Research Reviews Formerly: Current Drug Abuse Reviews. 2023 Nov 1;15(3):207-21.
19. Hossain MS, Jahan I, Islam M, Nayeem J, Anzum TS, Afrin NA, Mim FK, Hasan MK. Coccinia grandis: Phytochemistry, pharmacology and health benefits. Clinical Traditional Medicine and Pharmacology. 2024 Jun 1;5(2):200150.
20. Wasana KG, Attanayake AP, Weerarathna TP, Jayatilaka KA. Efficacy and safety of a herbal drug of Coccinia grandis (Linn.) Voigt in patients with type 2 diabetes mellitus: A double blind randomized placebo controlled clinical trial. Phytomedicine. 2021 Jan 1;81:153431.
21. Chavan S, Beldar AG, More RB. The anti-pathogenic activity and DNA gyrase inhibition of freshwater crabs (Barytelphusa cunicularis) are related to their structure-activity relationship. Bioorganic & Medicinal Chemistry Reports. 2024 Jul 1;7(2).
22. Chavan SV, Patil AA. Extraction, isolation and characterization of bioactive compound from tissue of fresh water crab Barytelphusa cunicularis from Northern Region of Maharashtra. International Journal of Innovative Science and Research Technology ISSN. 2021 Apr(2456-2165):6.
23. Giménez MJ, Aguilar L, Granizo JJ. Revisiting cefditoren for the treatment of community-acquired infections caused by human-adapted respiratory pathogens in adults. Multidisciplinary Respiratory Medicine. 2018 Dec;13:1-3.
24. Chavan S. V., Aquatic natural product chemistry, LAMBERT Academic Publishing, 2024.
25. Hanwell MD, Curtis DE, Lonie DC, Vandermeersch T, Zurek E, Hutchison GR. Avogadro: an advanced semantic chemical editor, visualization, and analysis platform. Journal of cheminformatics. 2012 Dec;4:1-7.
26. Krishnan RB. JS; Seeger, R.; Pople. J. Chem. Phys. 1980;72:650.
27. McLean AD, Chandler GS. Contracted Gaussian basis sets for molecular calculations. I. Second row atoms, Z= 11–18. The Journal of chemical physics. 1980 May 15;72(10):5639-48.
28. Blaudeau JP, McGrath MP, Curtiss LA, Radom L. Extension of Gaussian-2 (G2) theory to molecules containing third-row atoms K and Ca. The Journal of chemical physics. 1997 Oct 1;107(13):5016-21.
29. Curtiss LA, McGrath MP, Blaudeau JP, Davis NE, Binning Jr RC, Radom L. Extension of Gaussian-2 theory to molecules containing third-row atoms Ga–Kr. The Journal of Chemical Physics. 1995 Oct 8;103(14):6104-13.
30. Curtiss LA, McGrath MP, Blaudeau JP, Davis NE, Binning Jr RC, Radom L. Extension of Gaussian-2 theory to molecules containing third-row atoms Ga–Kr. The Journal of Chemical Physics. 1995 Oct 8;103(14):6104-13.
31. Kouza M, Banerji A, Kolinski A, Buhimschi I, Kloczkowski A. Role of resultant dipole moment in mechanical dissociation of biological complexes. Molecules. 2018 Aug 10;23(8):1995.
32. Hagar M, Ahmed HA, El-Sayed TH, Alnoman R. Mesophase behavior and DFT conformational analysis of new symmetrical diester chalcone liquid crystals. Journal of Molecular Liquids. 2019 Jul 1;285:96-105.
33. Khodair AI, Awad MK, Gesson JP, Elshaier YA. New N-ribosides and N-mannosides of rhodanine derivatives with anticancer activity on leukemia cell line: Design, synthesis, DFT and molecular modelling studies. Carbohydrate Research. 2020 Jan 1;487:107894.
34. Joshi R, Kumari A, Singh K, Mishra H, Pokharia S. Triorganotin (IV) complexes of Schiff base derived from 1, 2, 4-triazole moiety: Synthesis, spectroscopic investigation, DFT studies, antifungal activity and molecular docking studies. Journal of

Molecular Structure. 2020 Apr 15;1206:127639.R. Malhotra, A. Ravesh, V. Singh, *Phosphorus, Sulfur Silicon Relat. Elem.*, 192, **(2017)**, 1.

35. da Costa RM, Bastos JK, Costa MC, Ferreira MM, Mizuno CS, Caramori GF, Nagurniak GR, Simão MR, Dos Santos RA, Veneziani RC, Ambrósio SR. In vitro cytotoxicity and structure-activity relationship approaches of ent-kaurenoic acid derivatives against human breast carcinoma cell line. Phytochemistry. 2018 Dec 1;156:214-23.
36. Lewis DF. Quantitative structure–activity relationships (QSARs) within the cytochrome P450 system: QSARs describing substrate binding, inhibition and induction of P450s. Inflammopharmacology. 2003 Feb;11:43-73..
37. Al Sheikh Ali A, Khan D, Naqvi A, Al-Blewi FF, Rezki N, Aouad MR, Hagar M. Design, synthesis, molecular modeling, anticancer studies, and density functional theory calculations of 4-(1, 2, 4-triazol-3-ylsulfanylmethyl)-1, 2, 3-triazole derivatives. ACS omega. 2020 Dec 31;6(1):301-16.
38. Xavier S, Periandy S, Ramalingam S. NBO, conformational, NLO, HOMO–LUMO, NMR and electronic spectral study on 1-phenyl-1-propanol by quantum computational methods. Spectrochimica Acta Part A: Molecular and Biomolecular Spectroscopy. 2015 Feb 25;137:306-20.